JOURNAL OF MATERIALS PROCESSING TECHNOLOGY 209 (2009) 3705–3713

journal homepage: www.elsevier.com/locate/jmatprotec

Laser welding of Ti6Al4V titanium alloys

E. Akman, A. Demir, T. Canel, T. Sınmazçelik*

University of Kocaeli, Laser Technologies Research and Application Center, 41380 Umuttepe, Kocaeli, Turkey

ARTICLE INFO

Article history:
Received 21 May 2008
Received in revised form
27 August 2008
Accepted 28 August 2008

Keywords:
Laser seam welding
Laser material processing
Ti6Al4V titanium alloys

ABSTRACT

The high strength to weight ratio and excellent corrosion resistance of titanium alloys allow diverse application in various fields including the medical and aerospace industry. Several techniques have been considered to achieve reliable welds with minimum distortion for the fabrication of components in these industries. Of these techniques, laser welding can provide a significant benefit for the welding of titanium alloys because of its precision and rapid processing capability. For pulse mode Nd:YAG laser welding, pulse shape, energy, duration, repetition rate and peak power are the most important parameters that influence directly or synergistically the quality of pulsed seam welds. In this study, experimental work involved examination of the welding parameters for joining a 3-mm thick titanium alloy using the Lumonics JK760TR Nd:YAG pulsed laser. It has been determined that the ratio between the pulse energy and pulse duration is the most important parameter in defining the penetration depth. Also it has been observed the variation of pulse duration at constant peak power has no influence on the penetration depth. Consequently, to increase the penetration depth during welding, the role of the laser parameters such as pulse energy and duration and peak power have been investigated to join 3 mm thick Ti6Al4V.

1. Introduction

The low density, excellent high temperature mechanical properties and good corrosion resistance of titanium and titanium alloys have led to a diversified range of successful applications for the demanding performance and reliability requirements of the medical, aerospace, automotive, petrochemical, nuclear and power generation industries as reported by Wang et al. (2003) and Casalino et al. (2005). When the operation temperature exceeds 130 °C, titanium alloys can be used as replacements for aluminium-based materials to achieve improved mechanical properties at elevated temperatures for applications such as the external shells of turbines, the power units for avionics and the landing gear structural components in Boeings 747 and 757 as mentioned (Lima, 2005). Alternatively, as titanium is exhibit very low corrosion rates in human body fluids as demonstrated (Choubey et al., 2005), other applications that are relevant to the medical industry include prosthetic devices such as artificial heart pumps, pacemaker cases, heart valve parts as well as load bearing bone such as for hip bone replacement.

Although the welding procedures and equipment used for austenitic stainless steel and aluminium alloys can be applied in order to join commercially pure titanium and most of titanium alloys, their increased reactivity with atmospheric elements at high temperatures necessitates additional precautions to shield the molten weld pool as determined (Key to metals, 2006). Nonetheless, laser welding has considerable flexibility for joining titanium alloys either autogenously or with the use of filler wire or powder. As laser welding permits the generation of a keyhole that effectively concentrates the energy input into a small area, there is good potential to join titanium alloys since the microstructural changes are confined to the weld region and a narrow heat affected zone, which

* *Corresponding author*. Tel.: +90 262 3032915; fax: +90 262 3032915.
E-mail addresses: eakman29@gmail.com, erhan.akman@kou.edu.tr (E. Akman).
0924-0136/$ – see front matter © 2008 Elsevier B.V. All rights reserved.
doi:10.1016/j.jmatprotec.2008.08.026

has been reported to conserve the corrosion resistance and mechanical strength of the weldment (Liu et al., 2002).

To preserve the mechanical properties of titanium alloys during laser welding, gas shielding is of crucial importance to prevent embitterment of the weld region and the ensuing losses in ductility. Protection of the weld pool against atmospheric contaminations is performed by using shielding gas, which also has been reported to improve the coupling of the laser to the material (Wang et al., 2007). In order to enhance the coupling between the incident beam and the workpiece as well as prevent oxide formation on the weld surface, several laser welding nozzles have been developed. Conical nozzle has been designed by Gerevey et al. (2005) to stabilize the plasma plume that is used for obtaining good quality weld, ring nozzle has been designed to prevent contamination by the ambient air (Fabbro et al., 2004), and also a model has been employed by Ancona et al. (2006) describing the gas flow dynamics for coaxial conical nozzle. Examination of the influence of coaxial shielding gas or lateral assist gas on the laser welding process has indicated that the height of the side nozzle and current rate of gas flow can strongly influence weld seam characteristics. Specifically, Zhang et al. (2005a) have recently shown that, the largest weld bead width on the bottom surface is achieved when the joint angle of coaxial gas flow and side gas flow are at about 40°. To determine the effect of applying shielding protection with helium and argon gasses on titanium alloy using different nozzle designs, Caiazzo et al. (2004) have realized a study using CO_2 laser. As a result of this study, at constant power (1500 W), for each welding speed examined, a greater penetration depth has been obtained with helium gas than argon due to the lower ionization energy of argon that reduces energy transfer to the material. However, as well as the shielding gas used in laser welding protect the molten material from oxidation; it causes welding defects such as, porosity and cracks. The main reason of the porosity in welding process is the gas bubbles in the molten material that cannot escape before solidification. Doing the welding process in vacuum environment is an easy way to reduce the porosity problem. The effect of vacuum on weld penetration and porosity formation has been investigated on 304 stainless steel and A5083 Aluminium alloy by Katayama et al. (2001). The results have showed that vacuum welding has been effective in the prevention of porosity, no pores has been seen below 0.4 kPa and also penetration depth has increased and the fusion zone has become thinner with a decrease in pressure. Laser machining can replace mechanical removal methods in many industrial applications, particularly in the processing of difficult-to-machine materials such as hardened metals. Laser welding application of titanium alloys have been done by Akman et al. (2007), also Kacar et al. (2009) recently have shown that ceramics with 10 mm thicknesses can be drilled using high power laser. Among the high power density technologies, the electron beam and laser welding have showed a great capability in producing narrow and deep joints. The amount of heat used in laser welding is roughly comparable to that of conventional arc welding processes. As the heat is focused on a very small area, the weld pool is much smaller than in arc welding. As reported by Casalino et al. (2005), the welding speed is much higher, up to approximately the speed of conventional welding processes.

Table 1 – The composition of Ti6Al4V

Material	Content
C	<%0.08
Fe	<%0.25
N_2	<%0.05
O_2	<%0.2
Al	%5.5
V	%3.5
H_2	<%0.0375
Ti	Balance

To understand laser welding phenomena of commercially available pure titanium, the molten pool behaviour has been synchronously observed by Kawahito et al. (2006). By taking into consideration the relationship between the in-process monitoring signals and the welding results, the feasibility of adaptive control of laser peak power and pulse duration has been examined for reducing the spattering or porosity. Of the three welding techniques (TIG, Plasma and laser) compared to titanium alloys by Zheng et al. (2001), it has been reported that laser welds possess the highest aspect ratio and narrowest weld bead.

Titanium alloys can be welded using a pulsed and continuous wave (cw) mode laser. In pulsed laser applications, a small molten pool is formed by each laser pulse and within a few milliseconds it re-solidifies. When the peak power is low or the spot size is increased, welding occurs in conduction mode and a shallow and smooth weld pool is produced. On the other hand, when the peak power is increased or the spot size is reduced, a much deeper weld pool is obtained that is characterized as penetration or keyhole mode welding as reported (The fabricator, 2003). In keyhole mode laser welding, two plasmas, one inside the keyhole and other above the workpiece surface, occur. The plasma produced by laser radiation affects the welding process and an excess in the plasma has some disadvantages such as blocking, reflecting or refocusing the laser beam that can result in insufficient penetration, burn-through, irregular weld shape, or damage of beam delivery optics. As mentioned by Tu et al. (2003) and Zhang et al. (2005b) inside the keyhole, two absorption mechanisms usually exist in laser deep penetration welding: the beam energy is absorbed by the material through either Fresnel absorption of the keyhole wall during multiple reflections of the beam on the wall or the inverse Bremsstrahlung absorption of the electrons of the plasma. Although in continuous type lasers it is easier to control the laser welding processes, it has disadvantages for thin material processing.

Table 2 – Laser and systems parameters used in experiment

Parameter	Value
Pulse energy (J)	5.6, 6.5, 7.6, 8.5, 9.6, 10.5, 11.5, 12.5, 13.4
Pulse duration (ms)	5, 7, 10
Repetition rate (Hz)	43
Welding speed (mm/s)	5
Focal position (mm)	−2 mm
Gas pressure (bar)	1.5

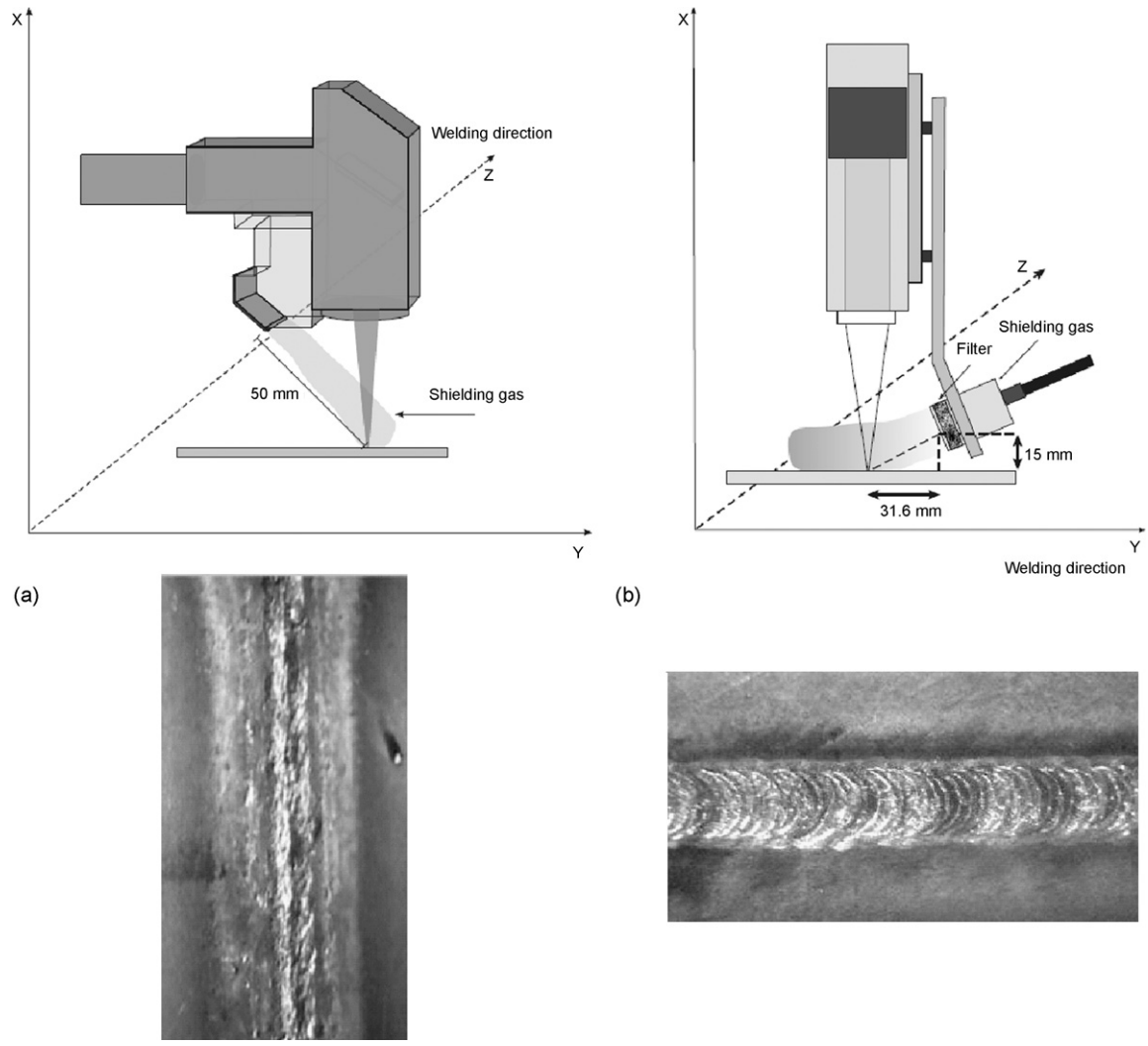

Fig. 1 – Shielding gas nozzle setups and oxidation effects.

Seam welding is the most important pulsed laser application. Tzeng (2000a) describes the seam welding as a series of overlapping spot welds to form a fusion zone or seam. The formation and the quality of seam welds are the results of a combination of various pulsed laser processing parameters, such as the travel speed, the average laser power, the pulse energy, the pulse duration, the average peak power density and the spot area. As mentioned by Tzeng (2000b), this abundance gives control of the thermal input with a precision not previously available and also permits a wide range of experimental conditions to be applied. On the other hand controlling so many parameters increases the complexity of laser processing. Lima (2005) has recently shown that pulse shaping technique can be used to prevent cracking in welded TiN coated titanium alloy through an improvement in the transfer of nitrogen to the volume of the weld. The optimum laser parameters and filler wire diameter are investigated by Li et al. (1997) in the welding process. Also the gap between the joint interfaces has been varied to evaluate porosity formation and/or reduction in the titanium alloy. They have shown that, acceptable results can be obtained when the gap distance is 0.1 mm. In this study, the effect of pulsed laser seam-welding parameters for joining 3 mm thick Ti6Al4V has been investigated using the Lumonics JK760TR pulsed Nd:YAG laser.

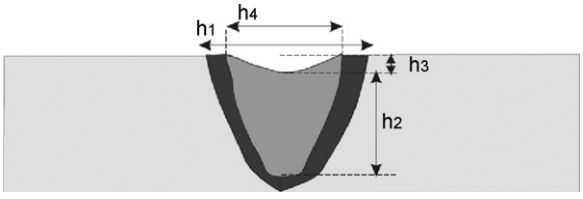

Fig. 2 – Characterization of welding cross-section.

2. Materials and methods

In this study, butt welding of a small square shaped (30 mm × 30 mm × 3 mm) Ti6Al4V titanium alloy plaques have been done using GSI lumonics JK760TR Series Laser (Class 4) system in a CNC cabin. The chemical composition in weight percentage of the titanium substrate is shown in Table 1. The JK760TR Series of laser is an Nd:YAG laser that has 0.3–50 ms

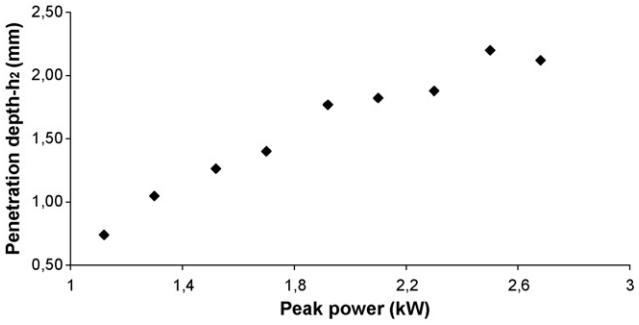

Fig. 3 – Effect of peak power on penetration depth.

pulse length and 500 Hz maximum repetition rate. The average power that can be obtained is 600 Watt. And also JK760 TR series laser has a pulse shaping ability. Laser output power is delivered via a 600-μm radius fiber optic cable to the focus head at the workstation for process. In the experiment, square shape pulse has been applied to all workpieces.

The laser beam is focused on titanium plates using 160 mm plano convex lens. The minimum spot size on the plates has been 0.4 mm. During welding application, the laser beam has been focused on 2 mm under the surface of the plates to obtain enough power density for the cross-section. In our case the spot size on the plates is 0.65 mm. The laser output parameters are varied in the experiment as Table 2.

There is always a cracking risk due to the rapid cooling of welded joint. To overcome this defect during welding, samples have been fixed on the ground using clamps. Titanium is reactive material at high temperature with ambient gases. For this reason during the welding application a shielding gas has been used to protect the melt pool and HAZ from oxidation until sufficient cooling has occurred. At this point shielding gas usage and nozzle set up are very important, formation of turbulence on the sample surfaces must be avoided. In experiments two different nozzle designs have been used. One of the nozzles has been arranged as array and formed by small sized gas exits and 5 bars helium applied during the experiment and 50 mm far from the welding area (see Fig. 1a). The second nozzle has 24 mm exit size and it has been kept to the weld area as close as possible and 1.5 bars helium gas has been applied (see Fig. 1b). In the second nozzle, to prevent the turbulences which might occur on the material surface wire filter has been used. The nozzle shown in Fig. 1b is used during the whole experiment phase since it prevents oxidation (see Fig. 1b). In Fig. 1b the overlapping spots welds are seen more clearly and the welding surface is shiny. The geometry of the welded cross-section gives very important information about the quality of the laser welding. The welded cross-sections of the materials are characterized by using four geometric parameters. The first one is called "h_1" and it represents the width of heat affected zone. The second depth is called "h_2" and it represents the penetration depth of the welding. The third depth is called "h_3" and it represents the dimensions of underfill defects. The fourth depth is called "h_4" and that one represents the width of weld pool. These distances are shown in Fig. 2.

The gap between the edges of the two workpieces is very important to prevent porosity formation. Therefore, before the welding process the edges of the workpieces have been made smooth as much as possible using milling cutter. The workpieces are clamped each other tightly in order to get the minimum gap formation between the edges and to reduce the breaking off risk during solidification. After welding application, cross-sections of workpieces have been prepared for optical microscopy using standard procedures including grinding, polishing and etching. And also the mechanical properties of the welded materials have been examined using tensile tests.

3. Results and discussion

Laser welding application begins with the determination of peak power which is the most important parameter affected on welding depth. Unsuccessful results can be obtained if the melt pool is too large or too small or if significant vaporization occurs during welding. Therefore, the control of laser power level as well as the pulse length is very critical. Penetration depth is increased with increase of peak power at constant pulse duration and spot diameter. Fig. 3 shows the cross-section of the welded specimens welded under the peak powers from 1.12 to 2.68 kW. During the welding, laser beam

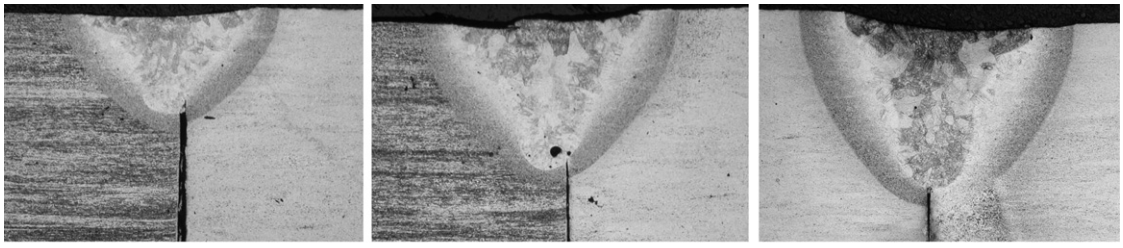

Peak Power = 1.12 kW
Pulse duration = 5 ms
h_1= 1,654 mm
h_2= 0,740 mm
h_3= 0 mm
h_4= 1,384 mm

Peak Power = 1.3 kW
Pulse duration = 5 ms
h_1= 1,945 mm
h_2= 1,047 mm
h_3= 0 mm
h_4= 1,489 mm

Peak Power = 1.7 kW
Pulse duration = 5 ms
h_1= 2,353 mm
h_2= 1,401 mm
h_3= 0 mm
h_4

Fig. 4 – Effect of peak power on penetration depth.

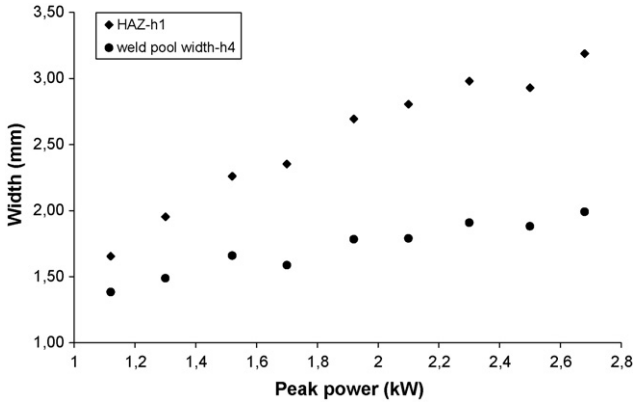

Fig. 5 – The effect of peak power on HAZ and weld pool width.

has been focused on 2 mm under from the surface and under these circumstances beam spot diameter is 0.65 mm on the surface of the workpiece. The pulse duration has been kept constant for each welding parameter as 5 ms.

As illustrated in Fig. 3, at lower laser power levels (approximately up to 2 kW) it has been found out that the penetration depths have increased linear with the peak power. This relationship changes after peak power of 2 kW and the depth of penetration (h_2) has been measured approximately constant around 1.8 mm. At higher peak power levels limitation at penetration depth increase is observed. This situation can be explained with plasma absorption of laser beam occurring in the keyhole. Not only the depth of penetration but also the heat affected zone (HAZ) and weld pool width are related to laser peak power. The plasma absorption is very strong at the top of the weld (at the surface of the material) where the available laser energy is high, this leads to enlarge the weld pool and HAZ width (see Figs. 4 and 5). The same effect has been reported by Weldingh and Kristensen (2001). The effects of peak power on penetration ability (h_2), weld pool (h_4) and HAZ (h_1) width are provided in Fig. 4.

At higher peak power levels the proportion between the HAZ and weld pool width is higher compared to low peak power levels. This situation can be explained by the transfer of more heat energy to keyhole walls with the increase of temperature inside the keyhole in high peak powers and advance of this heat with transmission deeper. The relationship between the peak power, HAZ and weld pool width is illustrated in Fig. 5.

The crater formation occurs at high peak power levels at the top of the surface labelled with "h_3". Highly focused energy is transferred by means of laser beam during the welding and this energy melts the material without vaporization. If the transferred energy is higher, the material loss comes up in weld pool and it is indicated as a crater formation with the

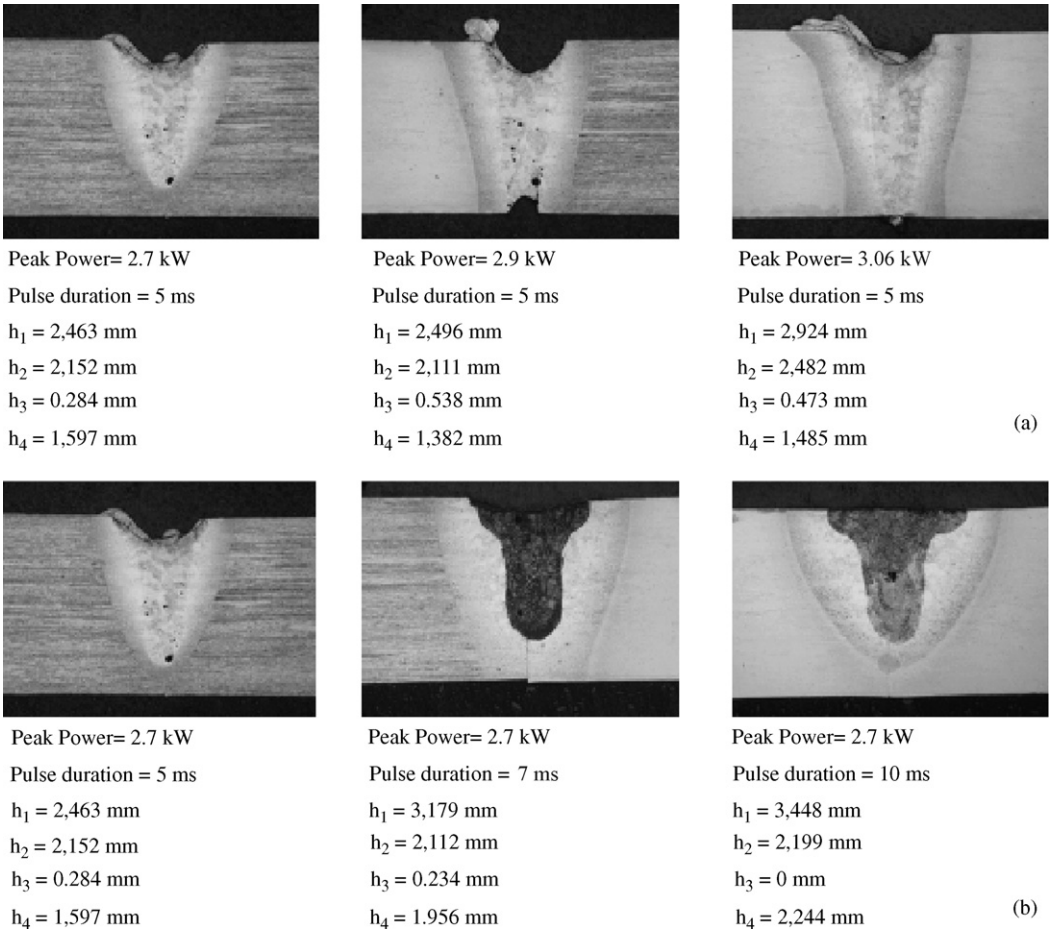

Fig. 6 – Effect of peak power on crater depth.

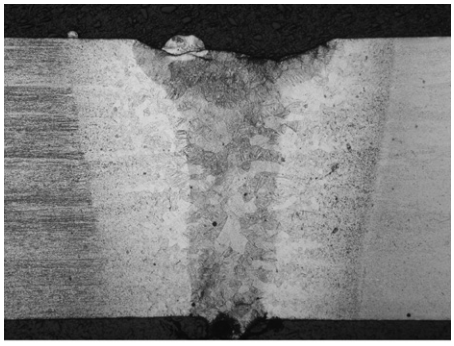

Fig. 7 – The deepest penetration has been obtained at 3 kW peak power and 10 ms.

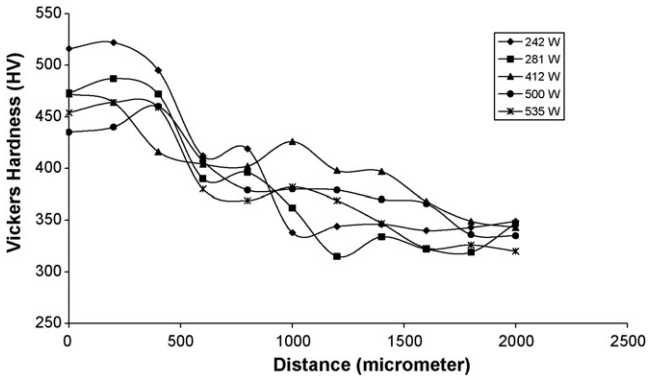

Fig. 9 – Micro-hardness distribution of workpieces for different average power.

depth of h_3 (Fig. 6a). In order to decrease the depth of these craters, the pulse duration has been increased at constant peak power. As seen in Fig. 6b the pulse duration effect on crater formation is illustrated and also as understood cross-section parameters in Fig. 6b at constant peak power, any increase on the pulse duration is not affected on penetration depth (h_2). But in this case due to longer interaction time between the laser pulse and the workpieces, wider weld pool and HAZ have been obtained. In Fig. 6 it is seen that there is porosity during welding process. The main reasons of the porosities are trapping of the some of the gases within the solidifying weld pool as determined (Kuo and Jeng, 2005). During the laser welding process formation and solidification of the melted material, hydrodynamic movements in the melted material (vortex formations) are the factors affected on size and dispersion of porosity. These are related to laser parameters (pulse energy, duration, shape, repetition rate, and peak power), type of assisting gas used and nozzle design. Pulse duration and the pulse energy have been increased in order to obtain deeper penetration without any loss on the surface. The deepest penetration has been obtained at 3 kW peak power and 10 ms pulse duration. It is illustrated in Fig. 7.

The hardness distributions of the welded cross-sections have been analyzed using a Zwick micro-hardness tester with a load of 300 g. The micro-hardness test has been carried out at 500 μm below the surface beginning on the centreline of the weld pool. As a result, at the centre of the weld pool the hardness is in the maximum level and the melted and cooled material is remarkable compared to the base metal due to its rapid cooling rate. The difference in hardness between the weld pool and the base metal is 140 HV. In heat affected zone, heating arises from the weld pool so the hardness is lower than the weld pool and the difference is 84 HV. The difference between the HAZ and the base metal is 56 HV. Different welding techniques are applied on Ti6Al4V alloys in literature. Electron beam, gas tungsten and laser welding techniques have been studied by Yunlian et al. (2000) to join the Ti6Al4V alloys and hardness differences between the base metal and the weld pool have been found 21, 41 and 150 HV, respectively. Another study is performed by Wanjara et al. (2006) using Electron beam, Tig and Laser welding techniques. The hardness differences between the base metal and the weld pool are 55, 37 and 180 HV, respectively. Previous works have shown that, high power density of laser beam welding provides a lower heat input and a more rapid solidification when compared to the conventional techniques, so laser welding technique leads to higher hardness values.

Any increase in the peak power produces lower heat input. It increases the target temperature producing steeper thermal

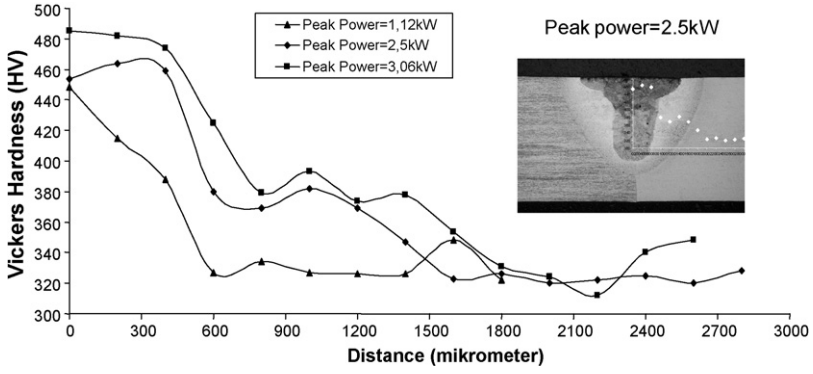

Fig. 8 – Micro-hardness distribution of three workpieces for different peak power.

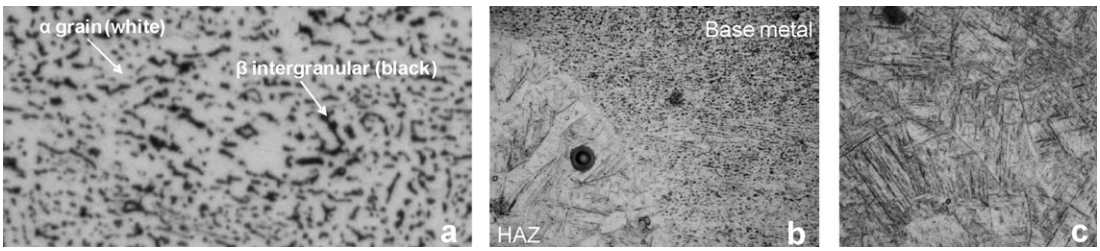

Fig. 10 – Microstructure of (a) base metal, (b) combination of HAZ and base metal, (c) Fuzion zone region.

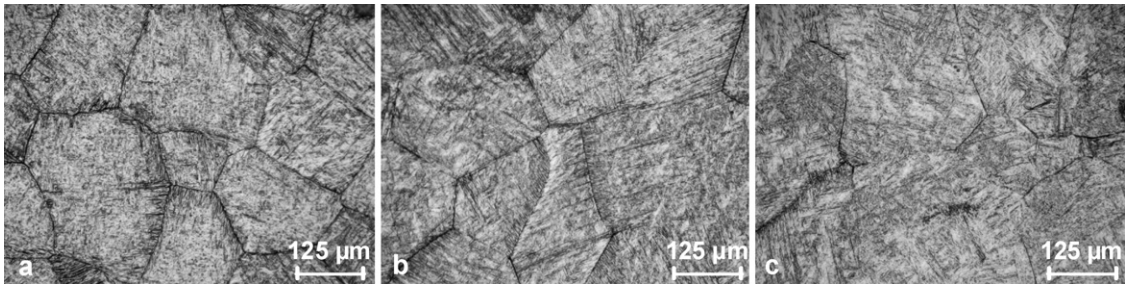

Fig. 11 – The effect of average power on grain size (a) 474 W, ~162.5 μm (b) 543 W, ~275 μm (c) 555 W, ~350 μm.

gradients and severe thermal straining. Whereas the increase in average power increases total heat input to the target reducing the cooling rate as well as the temperature gradient. So the hardness is likely to decrease with increasing average power. The same effect has been reported by Kumar (2006). The hardness distributions in the cross-section of the welded materials are illustrated in Fig. 8 as a function of peak powers and Fig. 9 as a function of average power.

The observed large increase in hardness in laser welded Ti–6Al–4V is due to high cooling rate associated with laser beam welding. The high cooling rates cause the formation of martensite in the weld zone HAZ region, this formation can be seen in Fig. 10b. It is reported by Sundaresan and Janaki (1999) that rapid cooling and subsequent martensitic transformation are effective strengthening methods for many Ti alloys.

Titanium-base materials have reversible transformation properties that crystal structure changes from alpha (hcp, hexagonal close-packed) structure to beta (bcc, body-cantered cubic) structure when the temperatures exceed to a certain level. Transition temperature is approximately 995 °C for Ti6Al4V alloy and it is called as beta transus temperature. This allotropic behaviour, which depends on the type and amount of alloy contents, allows complex alterations in microstructure and more diverse strengthening opportunities than those of the other nonferrous alloys as reported by Searles et al. (2005). In Fig. 10a optical microstructure of Ti6Al4V parent metal is shown. The structure consists of two phases: inter-granular beta phase (black) in an equaixed alpha phase (white). In Fig. 10b transition region from the HAZ to base metal is seen. The HAZ microstructure consists of a mixture of martensitic α', acicular α, and primary α. This kind of microstructure corresponds to a specimen quenched from a temperature below the beta transus. The martensitic α' transformed from the β grains, which corresponds to a structure quenched from the β phase above the beta transus, constitutes the microstructure of the fusion zone as mentioned by Smith (1993), as seen Fig. 10c.

As illustrated in Fig. 11, the grain size ascends with an increase in average power in both HAZ and weld metals. This is due to the heat-input increase at higher average power. Acicular martensites formed in columnar α (white) and β (black) grains in laser welded weld pool of Ti–6Al–4V alloy. Average grain size are 162.5, 275 and 350 μm for Fig. 11a, b and c, respectively. It should be kept in mind that the laser welding parameters have been selected as in Table 1. Each sample has been welded using 2.7 kW peak power.

Mechanical properties of the titanium alloys have been determined via tensile tests. Fig. 12 shows the design of specimens for tensile testing. Tensile testing has been performed at room temperature using a Zwick Roell tensile test machine operating with a cross-head speed of 10 mm/min with 50 kN load cell. The tensile strength of the original sample (unwelded) has been determined as 1066 N/mm^2. At work pieces seen in Fig. 13 peak power has been kept constant at 2.7 kW while pulse duration has been changed into 5, 7 and 10 ms. In this instance average power has changed into 336, 474 and 543 W, respectively. The h_1 values of the samples have varied as 2.463, 3.179 and 3.448 and h_2 values as 2.152, 2.112 and 2.119 for Fig. 13a, b and c, respectively. The tensile strength

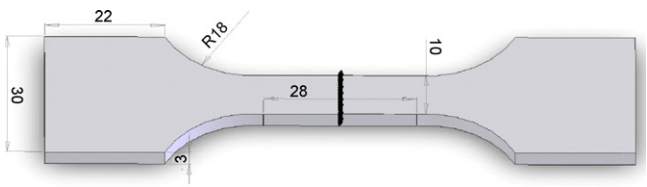

Fig. 12 – Schematic diagram of tensile test specimen design (mm).

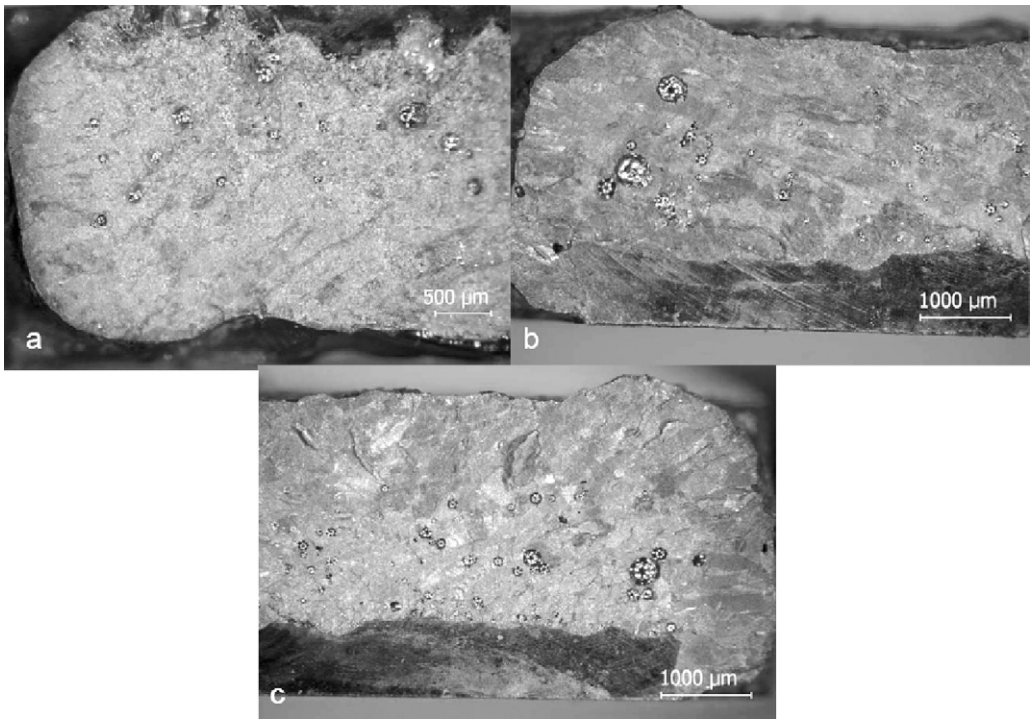

Fig. 13 – The cross-section of tensile test workpieces. Tensile strength are (a) 507.885 N/mm^2, (b) 145.29 N/mm^2, (c) 161.155 N/mm^2.

of this three samples have been determined as 507.885, 145.29 and 161.155 N/mm^2, respectively, although the depth of penetration (h_2) value (2.463) in Fig. 13a has been lower than the others but it has a higher tensile strength value compared to the others. The reason of this condition has been attributed to size of the porosities. In the measurements, porosity areas on Fig. 13a are quite fewer compared to the ones on Fig. 13b and c. The ratio between porosity areas and section areas as percentage has been calculated as %0.71, %2 and %2.083 in turn. The graphic of tensile test results related to the porosity ratio in welding area can be seen in Fig. 14. As a conclusion, it is possible to say that the microstructure and porosities are closely affected on the mechanical properties of the laser-welded materials.

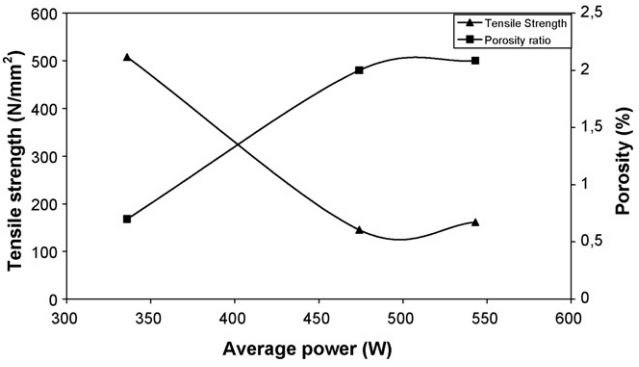

Fig. 14 – Tensile test results related to the porosity ratio in welding area, according to the average power variation.

4. Conclusions

The pulsed Nd–YAG laser welding technique has been employed to join Ti6Al4V titanium alloys. In general, the results show that it is possible to control the penetration depth and geometry of the laser weld bead by precisely controlling the laser output parameters. It has been seen that peak power is the most important parameter while determining the penetration depth which is equal to pulse energy per pulse duration. If the peak power is increased too much, the temperature of the workpieces exceeds to the evaporation point of the Ti6Al4V alloy, which promotes the crater formation on surface of the materials. To increase the penetration depth without craters, pulse duration is increased at constant peak power. When pulse duration is increased width of heat-affected zone, the weld pool will be increased at the same penetration depth. Because of the rapid cooling, the hardness of two welding zones is very high. The micro hardness profile across the weldment indicates that the hardness distribution in the fusion zone is higher than both the HAZ and parent metal. And also the hardness values are higher at high peak powers. Whereas the increase in average power increases total heat input to the target reducing the cooling and hardness values. The microstructure of the Ti6Al4V alloy has two phases. After the heat treatment microstructure of the alloys changes and it transforms from α to β phase. This transformation and growth in grain size is the reason for the decrease in tensile strength of the welded structures. Besides the change in microstructure, porosities which are caused by accumulated gases in melted material have a great effect on tensile strength.

Acknowledgement

This work has been supported by the University of Kocaeli Research Fund under 2004/33 project.

REFERENCES

Akman, E., Canel, T., Demir, A., Sinmazcelik, T., 2007. Optimization of pulsed Nd–Yag laser parameters for titanium seam-welding. AIP, Conf. Proc. 899, 303–304.

Ancona, A., Sibillano, T., Lugara, P.M., Gonnella, G., Pascazio, G., Maffione, D., 2006. An analysis of the shielding gas flow from a coaxial conical nozzle during high power CO_2 laser welding. J. Phys. D: Appl. Phys. 39, 563–574.

Caiazzo, F., Curcio, F., Daurelio, G., Memola, F., Minutolo, C., 2004. Ti6Al4V sheets lap and butt joints carried out by CO_2 laser: mechanical and morphological characterization. J. Mater. Process. Technol. 149, 546–552.

Casalino, G., Curcio, F., Memola, F., Minutolo, C., 2005. Investigation on Ti6Al4V laser welding using statistical and Taguchi approaches. J. Mater. Process. Technol. 167, 422–428.

Choubey, A., Basu, B., Balasubramaniam, R., 2005. Electrochemical behavior of Ti-based alloys in simulated human body fluid environment. Trends Biomater. Artif. Organs 18, 64–72.

Fabbro, R.A., Coste, F., Sabatier, L., Billion, J.P., 2004. US Patent US2004/0099643 A1.

Gerevey, D., Sallamand, P., Cicala, E., Ignat, S., 2005. Gas protection optimization during Nd:YAG laser welding. Opt. Laser Technol. 37, 647–651.

Kacar, E., Mutlu, M., Akman, E., Demir, A., Candan, L., Canel, T., Gunay, V., Sinmazcelik, T., 2009. Characterization of the drilling alumina ceramic using Nd:YAG pulsed laser. J. Mater. Process. Technol. 209, 2008–2014.

Katayama, S., Kobayashi, Y., Seto, N., Mizutani, M., Matsunawa, A., 2001. Effect of vacuum on penetration and defect in laser welding. J. Laser Appl. 13, 187–192.

Kawahito, Y., Kito, M., Katayama, S., 2006. In-process monitoring and adaptive control for laser spot and seam welding of pure titanium. J. Laser Micro/Nanoeng. 1, 269–274.

Key to metals, 2006. Welding of titanium alloys. http://www.Key-to-Metals.com.

Kumar, V.C., 2006. Process parameters influencing melt profile and hardness of pulsed laser treated Ti–6Al–4V. Surf. Coat. Technol. 201, 3174–3180.

Kuo, T.Y., Jeng, S.L., 2005. Porosity reduction in Nd–YAG laser welding of stainless steel and inconel alloy by using a pulsed wave. J. Phys. D: Appl. Phys. 38, 722–728.

Li, Z., Gobbi, S.L., Norris, I., Zolotovsky, S., Richter, K.H., 1997. Laser welding techniques for titanium alloy sheet. J. Mater. Process. Technol. 65, 203–208.

Lima, M.S.F., 2005. Laser beam welding of titanium nitride coated titanium using pulse-shaping. Mater. Res. 8, 323–328.

Liu, J., Watanabe, I., Yoshida, K., Atsuta, M., 2002. Joint strength of laser-welded titanium. Dent. Mater. 18, 143–148.

Searles, T., Tiley, J., Tanner, A., Williams, R., Rollins, B., Lee, E., Kar, S., Banerjee, R., Fraser, H.L., 2005. Rapid characterization of titanium microstructural features for specific modelling of mechanical properties. Meas. Sci. Technol. 16, 60–69.

Smith, W.F., 1993. Structure and Properties of Engineering Alloys, 2nd ed. McGraw-Hill, pp. 433–484.

Sundaresan, S., Janaki, R.G.D., 1999. Use of magnetic arc oscillation for grain refinement of gas tungsten arc welds in alpha–beta titanium alloys. Sci. Technol. Weld. Join. 4, 151–160.

The fabricator, 2003. When does laser welding become microwelding. www.thefabricator.com.

Tu, J.F., Inoue, T., Miyamoto, I., 2003. Quantitative characterization of keyhole absorption mechanisms in 20 kW-class CO_2 laser welding processes. J. Phys. D: Appl. Phys. 36, 192–203.

Tzeng, Y.F., 2000a. Process characterisation of pulsed Nd:YAG laser seam welding. Int. J. Adv. Manuf. Technol. 16, 10–18.

Tzeng, Y.F., 2000b. Parametric analysis of the pulsed Nd:YAG laser seam-welding process. J. Mater. Process. Technol. 102, 40–47.

Wang, H., Shi, Y., Gong, S., Duan, A., 2007. Effect of assist gas flow on the gas shielding during laser deep penetration welding. J. Mater. Process. Technol. 184, 379–385.

Wang, S.H., Wei, M.D., Tsay, L.W., 2003. Tensile properties of LBW welds in Ti–6Al–4V alloy at evaluated temperatures below 450 °C. Mater. Lett. 57, 1815–1823.

Wanjara, P., Brochu, M., Jahazi, M., 2006. Thin gauge titanium manufacturing using multiple-pass-electron beam welding. Mater. Manuf. Proc. 21, 439–451.

Weldingh, J., Kristensen, J.K., 2001. Very deep penetration laser welding—techniques and limitations. In: Proceedings of 8th NOLAMP Conference, Copenhagen, Denmark.

Yunlian, Q., Ju, D., Quan, H., Liying, Z., 2000. Electron beam welding, laser beam welding and gas tungsten arc welding of titanium sheets. Mater. Sci. Eng. A280, 177–181.

Zhang, L.J., Zhang, J.X., Wang, R., Yao, W., Gong, S.L., 2005a. Effects of side assist gas on the CO_2 laser welding process of thin stainless plate. Appl. Laser 25, 217–221.

Zhang, Y., Li, L., Zhang, G., 2005b. Spectroscopic measurements of plasma inside the keyhole in deep penetration laser welding. J. Phys. D: Appl. Phys. 38, 703–710.

Zheng, S., Dayou, P., Weihong, Z., Kuang, T. Y., 2001. Correlation between processing parameters and microstructures in tig, plasma and laser welded Ti–6Al–4V alloy. SIMTech Technical report.